ARTICLE
Pharmacology Discovery 2024;4(2):10. https://doi.org/10.53388/PD202404010

Comparative study of anti-inflammatory effects of different processed products through the COX-2/PGE2 signaling pathway: based on network pharmacology and molecular docking

Ping Chen[1, 2], Yun-Yun Quan[1, 2], An-Qi Zeng[1, 2], Ying Dai[1, 2], Jin Zeng[1, 2*]

[1]Translational Chinese Medicine Key Laboratory of Sichuan Province, Sichuan Academy of Chinese Medicine Sciences, Chengdu 610041, China. [2]Translational Chinese Medicine Key Laboratory of Sichuan Province, Sichuan Institute for Translational Chinese Medicine, Chengdu 610041, China.

[*]**Correspondence to:** Jin Zeng, Translational Chinese Medicine Key Laboratory of Sichuan Province, Sichuan Academy of Chinese Medicine Sciences, No. 51 Section 4, Renmin South Road, Chengdu 610041, China. E-mail: 466728392@qq.com.

Author contributions

Chen P and Zeng J designed this project, processed the samples, performed the experiments. Chen P wrote the article. Quan YY and Zeng AQ revised the article. Chen P analyzed the data. Chen P, Dai Y and Zeng J guided the experiment and provided funding for the research.

Competing interests

The authors declare no conflicts of interest.

Acknowledgments

This work was supported by Sichuan Province Science and Technology Support Program (NO. 2020JDJQ0063, NO. 2020YFS0566 and NO. 2021JDKY0037 (A-2021N-Z-5).

Peer review information

Pharmacology Discovery thanks Mohd Mukhtar Khan and other anonymous reviewers for their contribution to the peer review of this paper.

Abbreviations

FPP, Fu-zi Processed Products; RA, rheumatoid arthritis; LPS, lipopolysaccharide; TCM, traditional Chinese medicine; GO, Gene Ontology; PPI, protein-protein interaction; MF, molecular functions; BP, biological processes; CC, cellular components; KEGG, Kyoto Encyclopedia of Genes and Genomes; ELISA, enzyme-linked immunosorbent assay; SEM, standard error of the mean; ANOVA, analysis of variance.

Citation

Chen P, Quan YY, Zeng AQ, Dai Y, Zeng J. Comparative study of anti-inflammatory effects of different processed products through the COX-2/PGE2 signaling pathway: based on network pharmacology and molecular docking. *Pharmacol Discov*. 2024;4(2):10. doi: 10.53388/PD202404010.

Executive editor: Ting Yu.

Received: 22 March 2024; **Accepted:** 29 May 2024; **Available online:** 05 June 2024.

Abstract

Background: *Radix Aconiti Lateralis Preparata* (Fu-zi) is a traditional Chinese medicinal herb, which has been widely used in the clinic and has potent anti-inflammatory activities. we aimed to explore the mechanisms of extract containing alkaloids from different Fu-zi Processed Products (FPP) in treating inflammation, especially rheumatoid arthritis (RA). **Methods:** Firstly, using network pharmacology technology, the ingredients, and targets of Fu-zi were obtained by searching and screening, the targets involving RA were acquired, the intersection targets were constructed a "component-target-pathway" network. A comprehensive investigation was conducted on the anti-rheumatoid arthritis mechanisms of 5 FPPs in lipopolysaccharide (LPS) induced RAW264.7 cells, which serve as a model for RA. The production of NO and inflammatory cytokines were measured by ELISA kit. Quantitative Real-time PCR (qRT-PCR) was utilized to measure the mRNA levels. COX-2/PGE2 signaling pathway-associated proteins were determined by western blot. **Results:** According to a network pharmacological study, 16 chemical components and 43 common targets were found in Fu-zi and 6 key targets including PTGS2 were closely related to the mechanism of Fu-zi in treating RA. The *in vitro* study revealed that the levels of NO, TNF-α, and IL-1β were substantially decreased by the 5 FPPs. The 5 FPPs significantly suppressed the expression of proteins COX-2, iNOS, and NF-κB, with particularly notable effects observed for PFZ and XFZ. **Conclusion:** Altogether, these results demonstrated that the 5 PPS containing alkaloids have a good anti-RA-related inflammatory effect, and the mechanism may be related to COX-2/PGE2 signaling pathway, particularly, Fu-zi prepared utilizing a traditional Chinese technique.

Keywords: *Radix Aconiti Lateralis Preparata* (Fu-zi); rheumatoid arthritis; anti-inflammatory; network pharmacology; COX-2/PGE2 signaling pathway

Introduction

Inflammation represents the immune system's reaction to various stimuli, including biological agents, physical irritants, chemical substances, foreign materials, and necrotic tissue. Depending on the inflammatory process and cellular mechanisms involved, inflammation can be classified as either acute or chronic [1]. Acute inflammation, characterized by a short duration, local edema, and the migration of leukocytes, is a defensive response initiated by the rapid aggregation of immune cells at the site of injury. Chronic inflammation, in contrast to acute inflammation, is a slow and long-term form of inflammation that is primarily determined by the cause of injury and the body's ability to repair it. Chronic inflammation is also referred to as persistent low-grade inflammation. Unlike acute inflammatory reactions, chronic inflammation can persist for extended periods, ranging from weeks to months, or even be lifelong in the context of certain chronic inflammatory conditions [2]. Therefore, acute inflammation can develop into chronic inflammation due to persistent inflammation or poor repair [3–6]. Inflammatory response represents the primary cause for several diseases. Rheumatoid arthritis (RA) is a multifaceted and incapacitating autoimmune disorder that predominantly affects the joints, resulting in persistent inflammation, discomfort, and ongoing deterioration of joint structures. It is a long-term condition characterized by persistent inflammation, which can affect various systems in the body [7]. The most common lesion sites in RA are the small joints in the hands and feet, and are characterized by pain, swelling, and limited function. RA can cause cartilage damage, joint deformity, and even disability in severe cases [8]. Furthermore, individuals with RA tend to have a reduced lifespan compared to the general population, because of various comorbidities linked to the condition. The cause is attributed to heightened risk of cardiovascular issues, lung complications, infections, medical mishaps, or malignancies. Medications such as non-steroidal anti-inflammatory drugs (NSAIDs), corticosteroids, and disease-modifying anti-rheumatic drugs (DMARDs) are the commonly recommended drug to improve the clinical conditions of RA, although these drugs can exert some side effects [9, 10].

Radix Aconiti Lateralis Preparata, known as Fu-zi, is the processed form of the lateral root derived from *Aconitum carmichaelii Debx.*, a plant belonging to the Ranunculaceae family. Its use was initially documented in the " *Shennong's Materia Medica Classic* ", an ancient text revered as one of the foundational works in traditional Chinese medicine (TCM), where it is recognized as a frequently utilized remedy [11]. Fu-zi is poisonous and is therefore processed by a variety of specific techniques to reduce toxicity and maintain efficacy. Recent pharmacological research demonstrates that aconitine alkaloids are primarily responsible for the toxicity of fu-zi. In addition, previous research has shown that Fu-zi contains several alkaloids, primarily hypaconitine, aconitine, and benzoyl aconitine [12]. Fu-zi has been extensively utilized in the treatment of various ailments for over 2 millennia [13]. Clinically, Fu-zi is often used to treat a variety of diseases, such as RA, acute myocardial infarction, hypotension, coronary heart disease, chronic heart failure, tumor, skin trauma, depression, diarrhea, gastroenteritis and edema [14]. Research has proven that Fu-zi exerts notable anti-inflammatory, cardiotonic, analgesic and anti-aging effects. In prior research conducted by Luo et al., a network pharmacology approach was employed to identify the bioactive constituents and underlying mechanisms of Fu Zi Li Zhong Decoction with regards to the modulation of various pathways, such as those involved in cancer, the differentiation of Th17 cells, and the IL-17 signaling pathway [15]. In another study, Chen et al. discovered that Fu-zi possesses anti-inflammatory properties and can modulate the immune system, consequently decreasing the prevalence of allergic rhinitis and mitigating the nasal symptoms associated with allergic reactions [16]. Sun et al. combined Fu-zi with Ban-xia and found that this combination elicited concurrent protective effects on heart failure induced by pressure overload [17]. This protective effect was associated with suppression of the PKA/β2-AR-Gs signaling pathway. In another study, Feng identified that 25 bioactive compounds in Fu-zi acted holistically on 61 targets and 27 pathways in the treatment of RA and identified the regulation of inflammation regulation as one of the main mechanisms of Fu-zi [18]. Recently, Zhang et al. prepared gels containing epimedium polysaccharide components for RA treatment, demonstrating significant therapeutic efficacy and biosafety. It can also potentially reduce the systemic toxicity and irritation of oral administration of methotrexate, the first-line drug for RA, and can control the release of the drug for a long time [19].

Song reported that the activation of inflammatory response could occur *via* the regulation of cyclooxygenase 2 (COX-2)/prostaglandin E2 (PGE2) signaling [20]. Prostaglandin E2 (PGE2) is synthesized when arachidonic acid, liberated from the plasma membrane, undergoes enzymatic conversion by two cyclooxygenase enzymes (COX-1 and COX-2). Three different PGE2 synthase enzymes (PGEs) have been found to exert specific effects on the synthesis of PGE2 synthesis. Membrane bound microsomal prostaglandin E synthase-2 (mPGES-2) and cytosolic prostaglandin E synthase-1 (cPGES-1) are continuously expressed and are functionally associated with COX-1 to sustain the baseline levels of PGE2. Conversely, mPGES-1 is typically activated by diverse pro-inflammatory agents in conjunction with COX-2, leading to temporary surges in PGE2 concentrations [21].

Network pharmacology can systematically interpret the therapeutic effects of complex TCMs on diseases by analyzing the interaction between TCM components, targets, diseases, and pathways [22]. Monocytes and macrophages represent core components of innate immunity. Since macrophage-mediated inflammation is implicated in the regulation of RA, it is possible to use LPS-induced RAW264.7 macrophages to generate a model of RA [23, 24]. For the current investigation, we have utilized a network pharmacology strategy to dissect the underlying mechanisms by which Fu-zi Processed Products (FPPs) exert their therapeutic effects on RA. Furthermore, we carried out a comprehensive examination of FPP groups' anti-inflammatory effects in LPS-stimulated RAW264.7 cells, focusing on the COX-2/PGE2 signaling pathway. We hope that our findings could provide reference guidelines for the clinical application of Fu-zi to treat RA (Figure 1).

Materials and methods

Network pharmacology and molecule docking

Chemical compounds retrieving and active compounds screening. "Fu-zi" was searched and analyzed in TCMSP-Traditional Chinese Medicine Systems Pharmacology (https://tcmspw.com/tcmsp.php) and ETCM-The Encyclopedia of Traditional Chinese Medicine (http://www.tcmip.cn/ETCM/index.php/Home/) databases [25, 26]. In the TCMSP database, compounds were identified as active if they exhibited oral bioavailability (OB) of at least 30% and a drug-likeness (DL) score of no less than 0.18. The eligible active ingredients and protein targets were collected from these two data bases. Each active ingredient target was standardized using the Uniprot database (https://www.uniprot.org/), with the species specified as "*Homo sapiens*" [27].

Screening of disease-related genes. DisGeNet (https://www.Disgenet.org) database was used to retrieve RA related genes. Keywords "Rheumatoid Arthritis" were entered into the database and species were set as "Homo sapiens" to obtain disease-related gene targets. The potential targets associated with Fu-zi and RA were incorporated into the Venny 2.1 software. (https://bioinfogp.cnb.csic.es/tools/venny/index.html) for common targets.

Interaction analysis of protein-protein interaction (PPI). The shared targets obtained common targets were imported into STRING (https://cn.string-db.org/) database with parameters filtered by "*Homo sapiens*", and the confidence value was ≥ 0.4 [28]. Irrelevant nodes were hidden, and protein-protein interaction network graph was constructed, and Cytoscape 3.10.2 software was used for

visualization [29].

Enrichment analysis of GO and KEGG pathways. Metascape (https://metascape.org/gp/index.) data platforms were used to conduct GO and KEGG pathway enrichment analysis [30]. The human species, Homo sapiens, was selected for the study, and the results were analyzed by means of visual analysis. The Gene Ontology (GO) enrichment analysis encompassed the examination of molecular functions (MF), biological processes (BP), and cellular components (CC). Additionally, the Kyoto Encyclopedia of Genes and Genomes (KEGG) pathway enrichment analysis facilitated the identification of potential signaling pathways that Fu-zi may influence in the management of rheumatoid arthritis (RA).

Network construction. According to the above screened active ingredients, common targets, and main pathways, Cytoscape 3.10.2 software was used to construct a "component-target-pathway" network.

Molecule docking. Three-dimensional structural files for the ingredients, which were highly ranked in the predictive outcomes, were sourced from the PubChem database, available at https://pubchem.ncbi.nlm.nih.gov/. These ligand files were archived in the *Mol2 format. Concurrently, the crystallographic structures of the macromolecules were retrieved from the RCSB PDB, accessible at https://www.rcsb.org/, and stored in the *PDB format [31]. Subsequently, the ligand from the active site was dehydrated and eliminated using the PyMOL molecular visualization tool. The protein data file was loaded into AutoDock Vina for preparatory steps, which included the elimination of water molecules, the addition of hydrogen atoms, and the exportation in *pdbqt format. The drug molecule's rotatable bonds were configured and also saved in *pdbqt format. The position of the active site was constructed based on the coordinates of the original ligand. A grid box with specific spacing between grid points was defined to encompass the potential protein-binding region. The coordinates for the X, Y, and Z axes were aligned with the original ligand for various receptors. Ultimately, AutoDock Vina was utilized to perform the docking process and to identify the most favorable molecular conformation. The docking outcomes were subsequently imported into the PyMOL software for the purpose of visualization [32, 33].

Experimental verification

Preparation of sample. Fu-zi was collected from Butuo, Sichuan, and identified as the seed root of *Aconitum carmichaelii* Debx., a plant of the Ranunculaceae family, by Associate Researcher Zhou Xianjian of Sichuan Academy of Chinese Medicine Sciences. And all Fu-zi samples are stored in Sichuan Academy of Chinese Medicine Sciences. 5 methods were used for Fu-zi Processed Products (FPP): Fresh Fu-zi was obtained by washing the fresh Fu-zi and drying the surface moisture (SFZ); The ancient method of processing fresh Fu-zi was using grass and wood ash, which is fired until soft, peeled, sliced and dried at 60 ˚C to get processed Fu-zi (PFZ); Fresh Fu-zi was steamed at atmospheric pressure for 3 h, peeled, sliced, dried at 60 ˚C to get steam Fu-zi (ZFZ); Dried Fu-zi need to use fresh Fu-zi at 60 ˚C after baking at 150 ˚C for 3–6 h until soft (HFZ); Refer to the “Qianjinyao fang (Thousand golden essential prescriptions)”, famous ancient Chinese medical book, the preparation method of Fu-zi was to bury the fresh Fu-zi in the ash fire with embers and slowly cook it until it cracks, then remove the skin. Finally dried at 60 ˚C to get Fu-zi powder product (XFZ). 100 g of each Fu-zi Products was added with 10 times of water, extracted for 2 h and filtered. The extracts were combined twice, and the filtrate was concentrated to an appropriate amount to extract containing alkaloids.

Reagents and antibodies. The followings reagents were used: lipopolysaccharide (LPS) from Escherichia coli 055:B5 (L2880, Sigma-Aldrich, USA); dexamethasone (D137736, Shanghai Aladdin Biochemical Technology Co., Ltd, Shanghai, China). Antibodies against the following proteins were used: anti-NF-κB p65 (D14E12, Cell Signaling Technology, USA); anti-β-Actin (13E5, Cell Signaling Technology, USA); goat anti-rabbit IgG HRP (Cell Signaling Technology, USA); anti-COX2 (EPR12012, Abcam, USA); anti-iNOS(EPR16635, Abcam, USA); Animal Total RNA Isolation Kit (NO.RE-03014, Foregene, China); 5 × All-In-One Master Mix (with AccuRT Genomic DNA Removal kit) (G492, Applied Biological Materials Inc, Canada); EvaGreen Express 2 × qPCR Master Mix-No Dye (G891, Applied Biological Materials Inc, Canada); NO assay kit (S0021, Beyotime Institute of Biotechnology, China); Mouse IL-1β ELISA Kit (E-EL-M0044c, Elabscience Biotechnology Co., Ltd, China); Mouse IL-6 ELISA Kit (E-EL-M0044c, Elabscience Biotechnology Co., Ltd, China); Mouse TNF-α ELISA Kit (E-EL-M3063, Elabscience Biotechnology Co., Ltd, China); PGE2 ELISA Kit (ml037542 , Shanghai Enzyme-linked Biotechnology Co., Ltd, China).

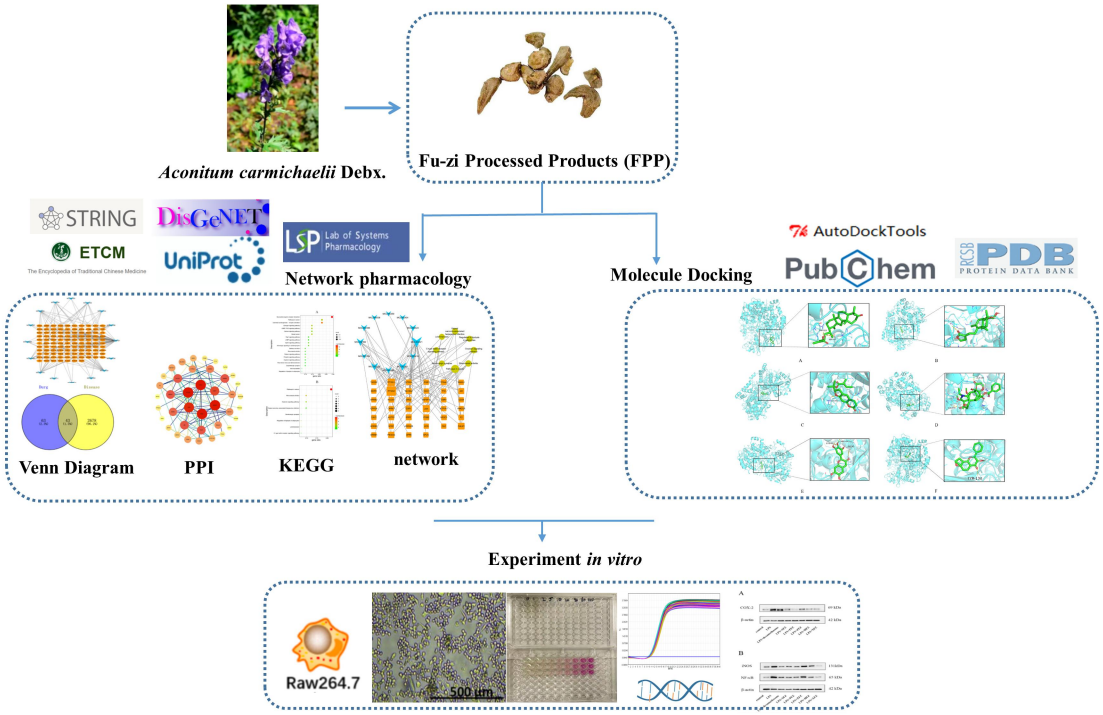

Figure 1 The experimental schematic of this research

Cell culture. The RAW264.7 murine macrophage cell line was procured from the Cell Source Center at the Chinese Academy of Sciences. The cells were cultivated in DMEM supplemented with 10% Fetal Bovine Serum (FBS), 100 U/mL penicillin, and 100 μg/ml streptomycin. They were kept at a temperature of 37°C in a humidified atmosphere containing 5% carbon dioxide.

Cell viability assay. A total of 5 × 10^3 RAW264.7 cells per well, suspended in 100 microliters of medium per well, were seeded into a 96-well plate. The plate was then incubated at 37 °C in a humidified chamber with an atmosphere of 5% CO_2. After 24 hours, the medium was discarded and FPPs (100 uL) and dexamethasone were added with different concentrations to each well, respectively. After incubation for 24 hours, cell viability was measured using a CCK-8 assay [34]. Subsequently, 10 μL of CCK-8 solution was added to each well, followed by incubation at 37 °C in an environment with 5% CO_2 for a duration of 1 to 4 hours. Ultimately, the absorbance in each well was measured at a wavelength of 450 nm employing a microplate reader. For each concentration, triplicate wells were prepared, and the entire experiment was conducted three times to ensure reproducibility. The concentration of FPPs and dexamethasone with cell viability over 90% were selected for subsequent experiments.

Nitric oxide (NO) production assay. Following overnight incubation in a 12-well plate with a density of 2 × 10^5 cells per well and a volume of 1000 μL of medium per well, the cells underwent a pre-treatment with lipopolysaccharide (LPS) for a duration of 1 hour. Then FPPs and dexamethasone were added for an additional 24 hours. The cells were observed under optical microscopy and the culture supernatant from each well was collected after centrifuge (2500 rpm, 20 minutes) and used to measure NO production. The NO levels were measured utilizing a commercially available NO detection kit, following the protocol provided by the manufacturer [35].

Cytokines production assays. Following overnight incubation in a 6-well plate with 1 × 10^6 cells per well and 2000 μL of medium per well, the cells were subjected to a one-hour pre-treatment with LPS. Then FPPs and dexamethasone were added for an additional 24 hours. The supernatant from the cell culture was harvested, and the concentrations of IL-1β, TNF-α and PGE2 secreted by the RAW264.7 cells were determined using a commercial enzyme-linked immunosorbent assay (ELISA) kit for mice, in accordance with the instructions provided by the manufacturer [36].

Total RNA extraction and qRT-PCR analysis. Following overnight incubation in a 6-well plate at a density of 1 × 10^6 cells per well with 2000 μL of medium per well, the cells underwent a 1-hour pre-treatment with LPS. The Trizol reagent was used to collect total RNA from the cells and stored in the refrigerator at −80 °C for later use. The process of reverse transcription was carried out following the guidelines provided with the reverse transcription kit, and the resulting complementary DNA (cDNA) was subsequently stored at a temperature of −20 °C in a refrigeration unit. The sequences of the primers used are shown in Table 1. According to the kit instructions, the housekeeping GAPDH served as an endogenous control, with each experimental sample being conducted in triplicate. The relative quantification of gene expression was identified using the comparative Ct ($2^{-\Delta\Delta Ct}$) method [34].

Western blot. After culture in a 6-well plate (1 × 10^6 cells/well, 2000 μL medium/well) overnight, the cells were pre-treated with LPS for 1 hour. Subsequently, FPPs and dexamethasone were introduced for a further 24-hour period. The cells were collected and subjected to lysis using a buffer solution that contained 250 mM sucrose, 50 mM NaCl, 20 mM Tris-HCl at a pH of 7.4, 1 mM EDTA, 1% Triton X-100, 1 mM DTT, and 1 mM PMSF, followed by incubation for 30 minutes in a cold environment. Following the incubation period, the cell lysates were subjected to centrifugation at 13,200 revolutions per minute (rpm) for a duration of 10 minutes. And then, the supernatants from each sample were carefully collected. The protein content was determined using the BCA assay reagents. The samples were then resolved by SDS-PAGE and subsequently electrophoretically transferred onto a PVDF membrane within a submerged transfer cell. Membranes were incubated with 5% non-fat dry milk powder dissolved in TBST for 3 times, 15 minutes each time. The membranes were immersed in primary antibody solutions and allowed to incubate for an extended period (overnight) at a temperature of 4 °C within a shaking incubator to ensure uniform exposure. Post incubation, the membranes underwent three rounds of washing with TBST to remove unbound antibodies. Following the washes, the membranes were incubated for a period of one hour at ambient temperature with secondary antibodies conjugated to peroxidase, which had been appropriately diluted in a blocking solution. Once the incubation with the secondary antibodies was complete and another series of washes performed, the detection of proteins was achieved using an ECL detection kit [34].

Statistical analysis. The data are displayed as the mean value accompanied by the standard error of the mean (SEM) derived from separate experiments. The statistical analysis of the outcomes was executed using one-way analysis of variance (ANOVA). The *P*-value of 0.05 or lower was deemed to indicate statistical significance.

Results

Screening of chemical constituents and targets and the identification of disease-related genes

By screening TCMSP and ETCM databases, we identified 16 chemical components of Fu-zi after removing non-target components. Matching protein targets were identified by the Uniprot database and 107 targets of the chemical components of Fu-zi were formally identified following the removal of duplicates. Data were subsequently loaded into the Cytoscape software, where an active ingredient-target interaction network was created. The DisGeNET database identified 2721 RA-related genes after removing duplicates. The targets of Fu-zi were then intersected with the RA-related genes, and 43 important targets for the treatment of RA were identified (Figure 2).

Identification of key targets of Fu-zi for RA and disassembly of PPI network modules

The PPI network was constructed utilizing the STRING database, and the Cytoscape software was employed to visualize the network. The network comprised 41 nodes and 122 connections. The degree of each node was calculated, and the target point size was scaled based on the degree values, with the top 6 nodes being PTGS2, NR3C1, CAV1, ESR1, JUN, and CNR1 (Figure 3).

Table 1 The primers utilized in the qRT-PCR research

Gene	Sequence (5′ to 3′)
GAPDH	F:GGTTGTCTCCTGCGACTTCA
	R:TGGTCCAGGGTTTCTTACTCC
COX-2	F:CTGGTGCCTGGTCTGATGATGTATG
	R:GGATGCTCCTGCTTGAGTATGTCG

Pharmacology Discovery 2024;4(2):10. https://doi.org/10.53388/PD202404010

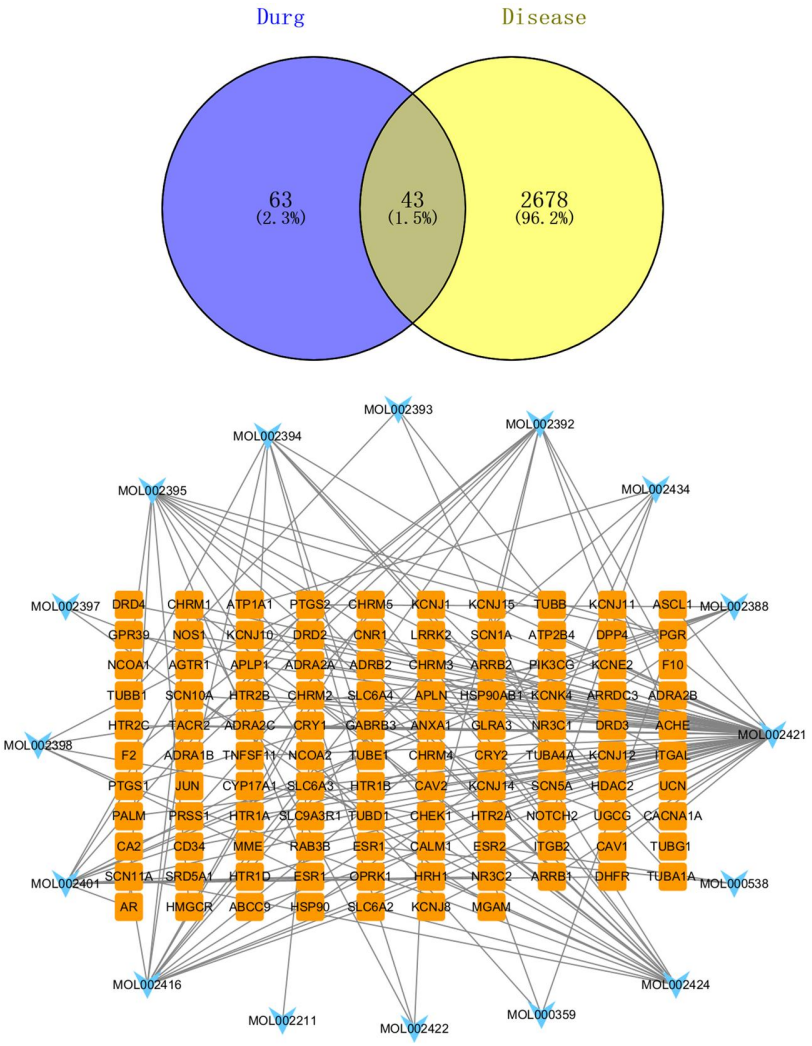

Figure 2 Venn diagram showing Fu-zi targets, RA targets, and the active ingredient-target network

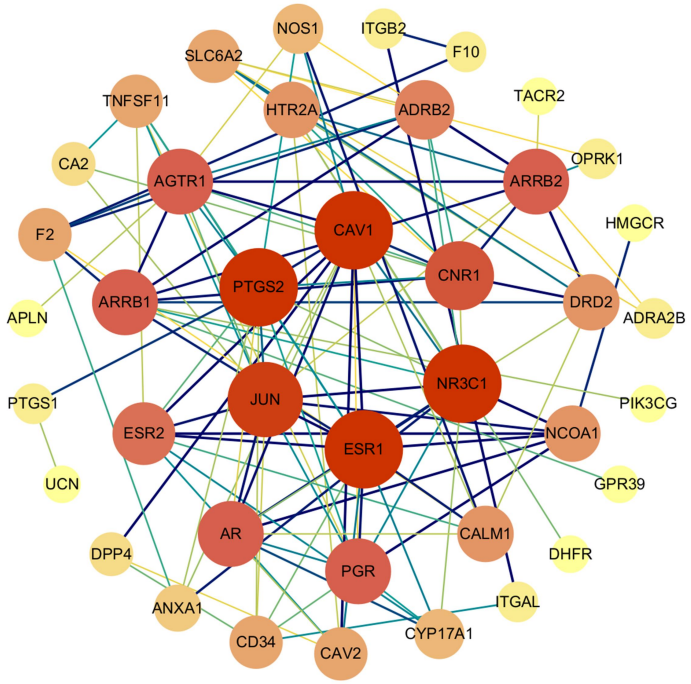

Figure 3 A PPI network was created to depict the connections among the Fu-zi targets. Any nodes that did not have connections to other nodes were removed from the network.

Pharmacology Discovery 2024;4(2):10. https://doi.org/10.53388/PD202404010

Enrichment analysis of the nodes of Fu-zi acting on RA and the generation of an ingredient-target-pathway network

Metascape was employed to conduct GO functional enrichment analysis and KEGG pathway enrichment analysis for the 41 target genes linked to the therapeutic effects of Fu-zi on RA. The GO analysis yielded a total of 477 biological processes (BPs), 55 cellular component (CCs) and 44 molecular functions (MFs). The first 10 components of each functional item are presented as a bar chart in Figure 4. A total of 46 pathways were identified by KEGG pathway enrichment analysis. The top 20 pathways with *P* values are shown as a bubblemap in Figure 5A. Of these, three pathways were related to PTGS2: pathways in cancer, the oxytocin signaling pathway, and the regulation of lipolysis in adipocytes. In addition, we screened KEGG pathways related to PTGS2 and RA, and identified eight key pathways, as shown as a bubble-map in Figure 5B. According to these findings, relevant data were imported into Cytoscape 3.10.2 to construct a tripartite network featuring the key ingredients and targets (Figure 6). This analysis predicted that target PTGS2 (also known as COX-2) served as a crucial factor in the effects of Fu-zi on RA. and the chemical components of Fu-zi with the values of degree No.2 to No.7 were all related to target PTGS2. Thus, the COX-2/PGE2 pathway was used as the basis for the next part of our study. The network characteristic parameters of the top 10 components and targets of Fu-zi in the treatment of RA are given in Table 2 and 3.

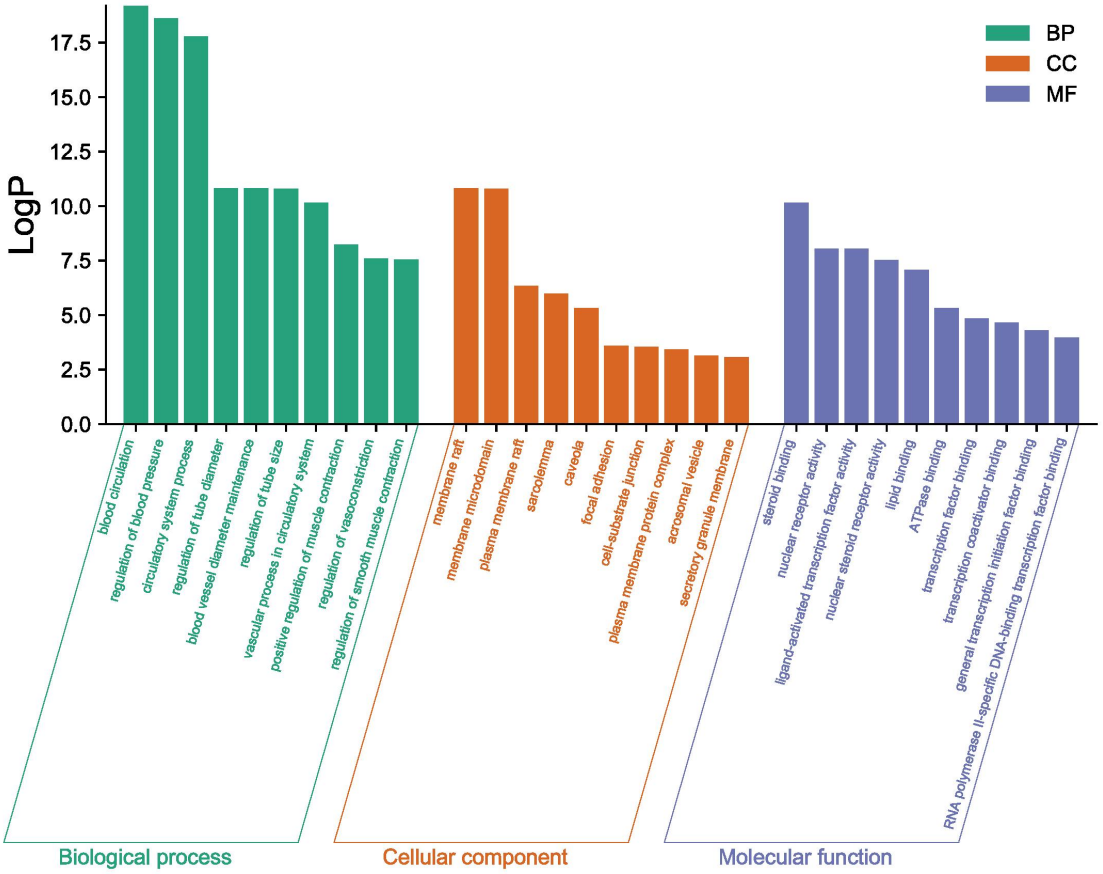

Figure 4 Results of GO function enrichment analysis

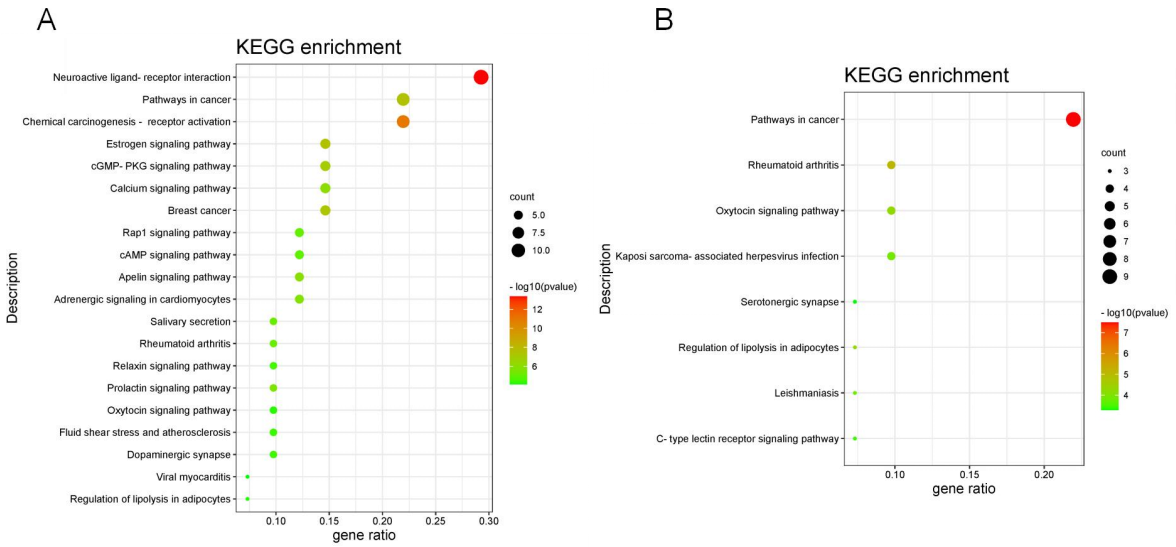

Figure 5 Results of KEGG pathway enrichment analysis

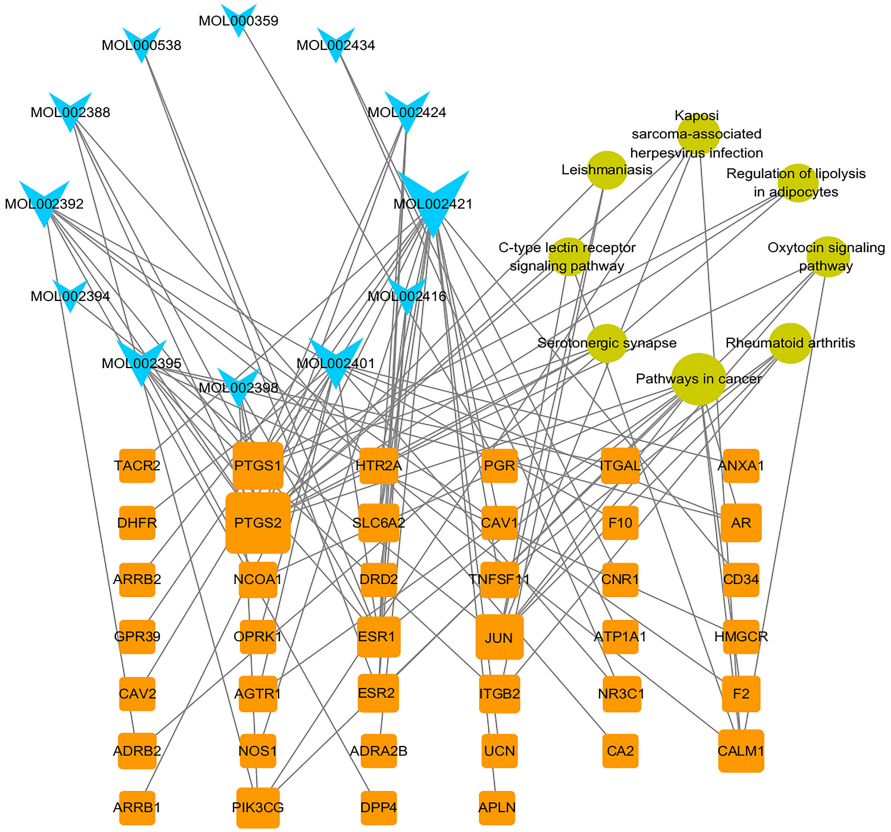

Figure 6 The ingredient-target-pathway network was visualized. The node size was directly proportional to their connectivity, signifying that larger nodes hold greater significance within the network.

Table 2 Parameters of main components

Molecule ID	Ingredient	Degree	Betweenness centrality	Closeness centrality
MOL002421	Ignavine	16	0.41525019	0.30366492
MOL002401	Neokadsuranic Acid B	9	0.22698497	0.33142857
MOL002395	Deoxyandrographolide	7	0.09974108	0.32402235
MOL002392	Deltoin	7	0.10824436	0.31693989
MOL002424	Aconitine	5	0.24320265	0.37908497
MOL002388	Delphin_qt	4	0.04321747	0.30687831
MOL002398	Karanjin	4	0.01735656	0.30687831
MOL002416	Deoxyaconitine	3	0.01535592	0.25777778
MOL000538	Hypaconitine	2	2.0165E-4	0.22222222
MOL002434	Carnosifloside I	2	0.03448276	0.204947

Table 3 Parameters of main targets

Target	Degree	Betweenness centrality	Closeness centrality
PTGS2	13	0.41339915	0.42028986
PTGS1	7	0.15340418	0.35365854
JUN	6	0.6076305	0.31182796
CALM1	5	0.01429188	0.27102804
ESR1	4	0.02088517	0.28431373
PIK3GC	4	0.00455187	0.2815534
ESR2	3	0.02427945	0.3333333
SLC6A2	3	0.17269302	0.2900000
ITGB2	3	0.01808496	0.27884615
AR	3	0.01461805	0.27619048

Pharmacology Discovery 2024;4(2):10. https://doi.org/10.53388/PD202404010

Verification with molecular docking

Molecule docking was performed to further identify the potential effects of 6 ingredients which were related to target PTGS2 of Fu-zi on RA, including Neokadsuranic Acid B, Deoxyandrographolide, Deltoin, Aconitine, Delphin_qt and Karanjin. As known that the binding energy ≤ -5.1 kcal/mol, an increased likelihood of their integration, coupled with enhanced stability of the ligand-macromolecule complex. Docking analysis successfully predicted binding energy, which the binding energy were all ≤ -5.1 kcal/mol, between PTGS2 and the 6 ingredients. At the same time, all RSMD values are less than 0.5 (nm) indicating stability.

The results are listed in Table 4. Overall, molecular docking results indicated that the 6 ingredients had good binding activities to PTGS2, as shown in Figure 7.

Effects of different FPPs and dexamethasone on the viability of RAW264.7 cells

CCK-8 assays indicated that dexamethasone did not exert any significant cytotoxic impact under the experimental conditions utilized in our research (Figure 8A). However, the FPPs exerted significant cytotoxic effects on RAW264.7 macrophages at a concentration of 40 mg/mL ($P < 0.001$) (Figure 8B–8F). Based on the experimental requirements and results, the selected concentrations of dexamethasone and Fu-zi were 0.8 mg/mL and 20 mg/mL, respectively.

Table 4 Docking simulation for active molecular and targets of RA

Molecular name	Targets	PBD ID	amino acid residue involved in H bonding	Binding energy (kcal/mol)	RSMD (nm)
Neokadsuranic acid B	PTGS2	5F19	TRP-323, ER-49	−8.5	0.001
Deoxyandrographolide	PTGS2	5F19	TYR-373	−8.2	0.057
Deltoin	PTGS2	5F19	GLN-461	−9.0	0.128
Aconitine	PTGS2	5F19	ALA-543, LN-370	−8.0	0.093
Delphin_qt	PTGS2	5F19	CYS-41, ARG-44, CLY-45	−9.3	0.090
Karanjin	PTGS2	5F19	TYR-130	−9.8	0.000

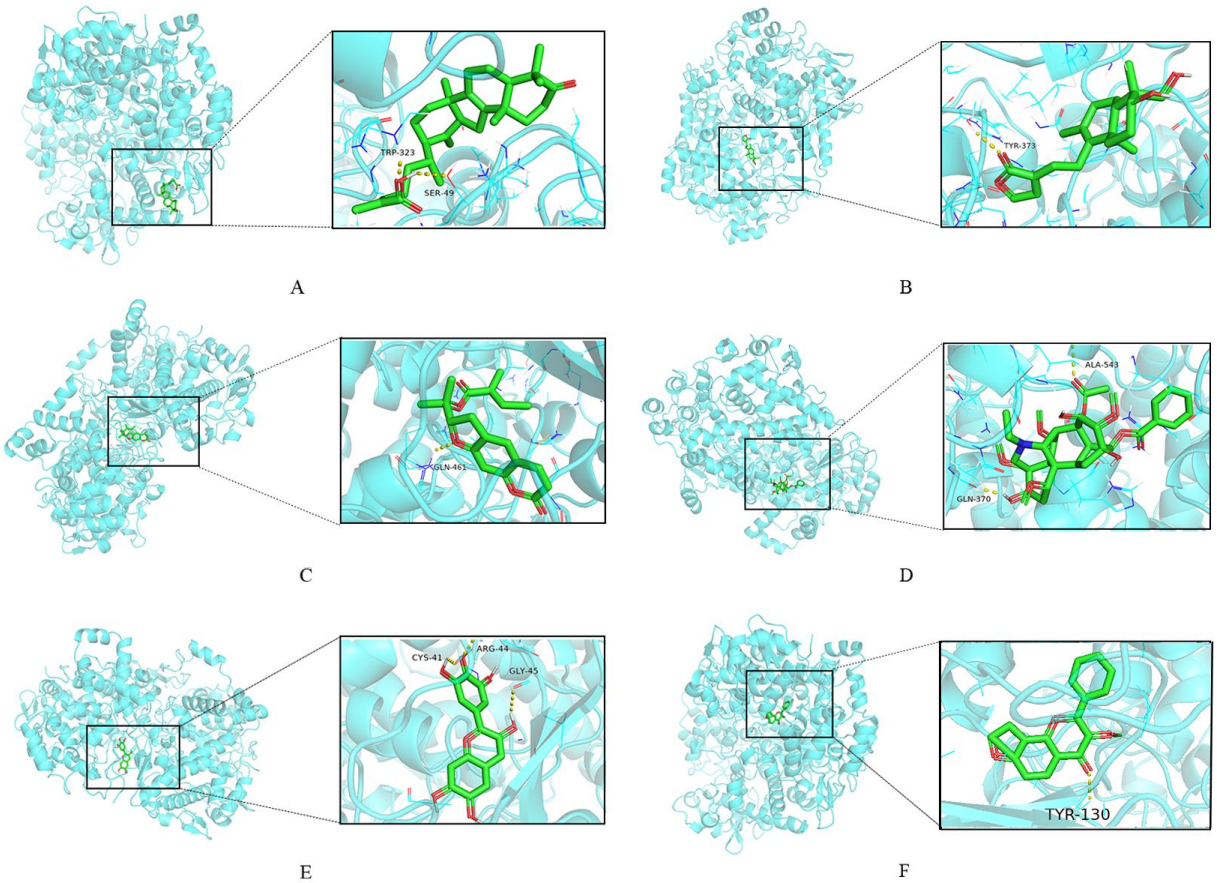

Figure 7 Molecule docking results of the main active components and the key target PTGS2. (A) Neokadsuranic Acid B binds to protein PTGS2. (B) Deoxyandrographolide binds to protein PTGS2. (C) Deltoin binds to protein PTGS2. (D) Aconitine binds to protein PTGS2. (E) Delphin_qt binds to protein PTGS2. (F) Karanjin binds to protein PTGS2.

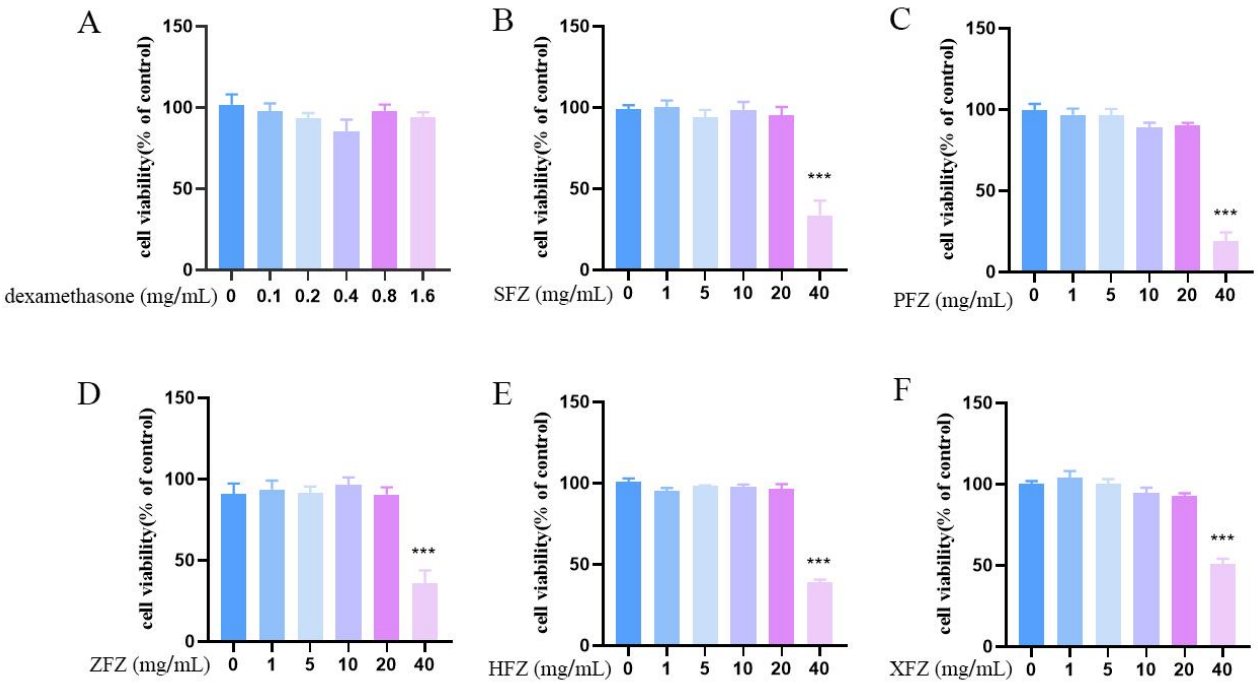

Figure 8 Cell viability of different FPPs and dexamethasone cultured in RAW264.7 macrophages. (A) Dexamethasone. (B) SFZ. (C) PFZ. (D) ZFZ. (E) HFZ. (F) XFZ. The assessment of cell viability was conducted using the CCK-8 assay, in accordance with the procedures detailed in the Materials and Methods section. The data are presented as means ± SEM (n = 3). ($^{***}P < 0.001$ vs. control group).

Effects of different FPPs on LPS-induced NO, IL-1β, IL-6, TNF-α and PGE2 production by RAW264.7 cells

Next, we observed the morphology of cells in each group by optical microscopy and found that the RAW264.7 cells in the untreated control group exhibited a rounded shape with smooth edges and lacked pseudopodia. In contrast, cells stimulated with LPS underwent significant differentiation (Figure 9A–9B). After exposure to FPPs and dexamethasone, the alterations in cellular morphology were mitigated in a dose-dependent fashion (Figure 9C–9H). To explore the anti-inflammatory effects of the FPPs, LPS was employed to induce the secretion of NO, IL-6, and TNF-α in RAW264.7 cells, thereby creating a setting that mimics chronic inflammation. The LPS stimulation of RAW264.7 cells for 24 hours induced inflammation and a significant increase in the significant secretion of NO, IL-6, and TNF-α in the supernatant. However, the five FPPs notably attenuated the release of these cytokines. Notably, there were differences in terms of anti-inflammatory effects when compared between the 5 FPP processing methods. For example, in the LPS group, there was an increased production of NO compared to the control group. It was also determined that HFZ was more potent in terms of its inhibitory effect on NO generation provoked by LPS (Figure 10A). LPS significantly increased levels of the pro-inflammatory cytokines IL-1, TNF-, and PGE2. In contrast, treatment with PFZ and ZFZ at a dose of 20 mg/mL significantly inhibited the levels of IL-1β, TNF-α and PGE2. In contrast to the LPS group, the concentrations of inflammatory cytokines (IL-1β and TNF-α) within LPS-induced FPP groups were notably diminished (Figure 10B–10C). Compared with the LPS group, the levels of PGE2 were significantly reduced, although there was no difference between HFZ and XFZ (Figure 10D). Our results indicate that FPPs possess anti-inflammatory capabilities by suppressing the generation of NO and various pro-inflammatory cytokines, including IL-1β, TNF-α, and PGE2, in RAW264.7 cells treated with LPS. There were differences in anti-inflammatory effects and further studies are now needed to determine which FPP is better.

Effects of different FPPs on LPS-induced expression of the COX-2 gene

According to the above results, PTGS2 is an important target of Fu-zi in the inflammatory response, especially in RA. PTGS2, also known as cyclooxygenase 2 (COX-2), is an important rate-limiting enzyme in prostate metabolism and leukotriene metabolism. It is well known that prostaglandins and leukotrienes are important mediators of inflammation. To investigate the anti-inflammatory effect of different FPPs on LPS-treated RAW264.7 cells, qRT-PCR was performed to measure the mRNA expression of COX-2. As shown in Figure 11, overproduction of COX-2 was typically observed in RAW264.7 cells after stimulation with LPS for 24 h. As expected, COX-2 levels were significantly and differentially reduced by different FPPs (Figure 11). Compared with other groups, the expression of COX-2 mRNA in the XFZ group was significantly decreased under the same concentration.

Effects of different FPPs on LPS-induced expression of NF-κB, COX-2 and iNOS proteins

Figure 12 illustrates that the levels of COX-2, iNOS, and NF-κB protein expression were notably elevated in the LPS group relative to the control group ($^{\#\#\#}P < 0.001$ vs. control group). In contrast to the LPS group, there was a significant decrease in the expression levels of COX-2 and iNOS proteins within the FPP groups treated with LPS ($^{*}P < 0.05$, $^{**}P < 0.01$ and $^{***}P < 0.001$ vs. LPS group). In addition, compared with the LPS group, the expression levels of NF-κB protein were significantly reduced in the LPS-induced FPP groups except for the ZFZ group ($^{*}P<0.05$, $^{**}P< 0.01$ and $^{***}P < 0.001$ vs. LPS group). On the other hand, the expression levels of COX-2, iNOS, and NF-κB proteins were significantly reduced in PFZ and XFZ groups when compared with other FPP groups at the same concentration.

Discussion

Fu-zi, a widely utilized herb in traditional Chinese medicine, has a history spanning more than 2,000 years, during which it has been employed to alleviate joint discomfort and manage rheumatoid conditions. Although fu-zi has toxicological risks, it still has a very high utilization rate in the clinical application of TCM [37]. The fresh fu-zi was processed by the Chinese traditional processing method to

guarantee clinical safety and minimal toxicity. The efficacy of old classical prescriptions has been impacted by changes in the Fu-zi processing system since antiquity [38]. Alkaloids of aconite are the main potent substances of the herb; of these, the diester type alkaloids (aconitine, mesaconitine, and hypacaonitine) are highly toxic components, while the monoester type alkaloids (benzoyl aconitine, benzoyl neoaconitine and benzoyl hypaconitine) are active components [39]. To verify the reliability of the processing methods of Fu-zi in ancient Chinese classical recipes, this study incorporated network pharmacology and compared the anti-inflammatory effects of five FPPs, including the ancient processing method. In this study, we found that 6 ingredients , including Neokadsuranic Acid B, Deoxyandrographolide, Deltoin, Aconitine, Delphin_qt and Karanjin, are the main potent substances related to RA. The 6 active ingredients involved in molecular docking were searched for inflammation-related content through sites such as PubChem (https://pubchem.ncbi.nlm.nih.gov/). The anti-inflammatory effects of the other five active components were reported except for Neokadsuranic Acid B. Deoxyandrographolide can exert anti-inflammatory effects through the COX-2 (PTGS2)-related pathway is the active component there, which is in agreement with our molecular docking results [40]. It has been shown that Deltoin are potential NO production inhibitor, which may explain the reduction of NO expression in LPS-induced macrophage RAW264.7 by appendicitis in this paper [41]. Aconitine also showed its anti-inflammatory effect and analgesic effect in animal experiments [42]. In addition, Delphin reduced the expression of pro-inflammatory factors such as IL-1β and TNF-α in LPS-induced macrophages RAW264.7 to alleviate inflammatory symptoms [43]. Similarly, Karanjin is involved in the secretion of the major pro-inflammatory cytokine TNF-α by macrophages involved in joint inflammation and destruction, and these are also indirectly demonstrated in the cellular experimental results and molecular docking results herein [44].

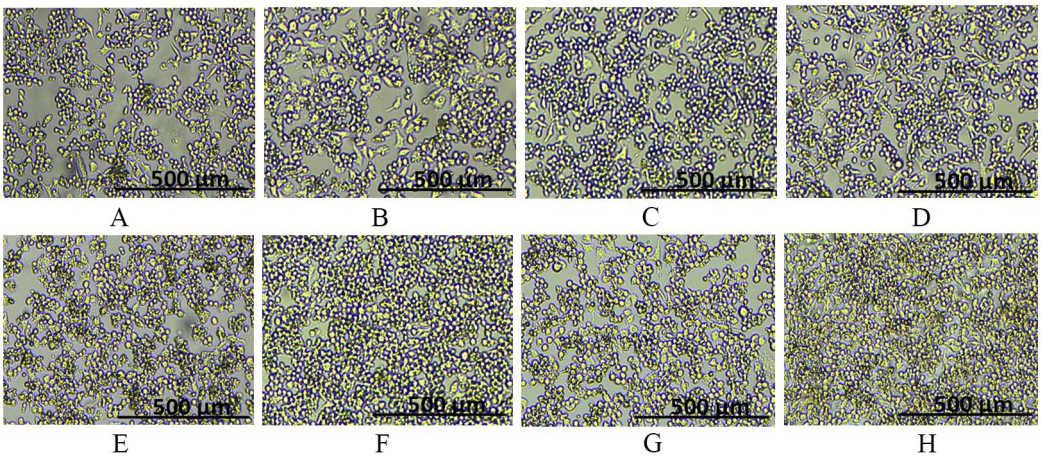

Figure 9 Images of RAW264.7 cells exposed to LPS for an additional 24 hours were captured using a light microscope at a magnification of 40x. (A) Control. (B) LPS. (C) LPS and dexamethasone. (D–H) LPS and Fu-zi (SFZ, PFZ, ZFZ, HFZ and XFZ).

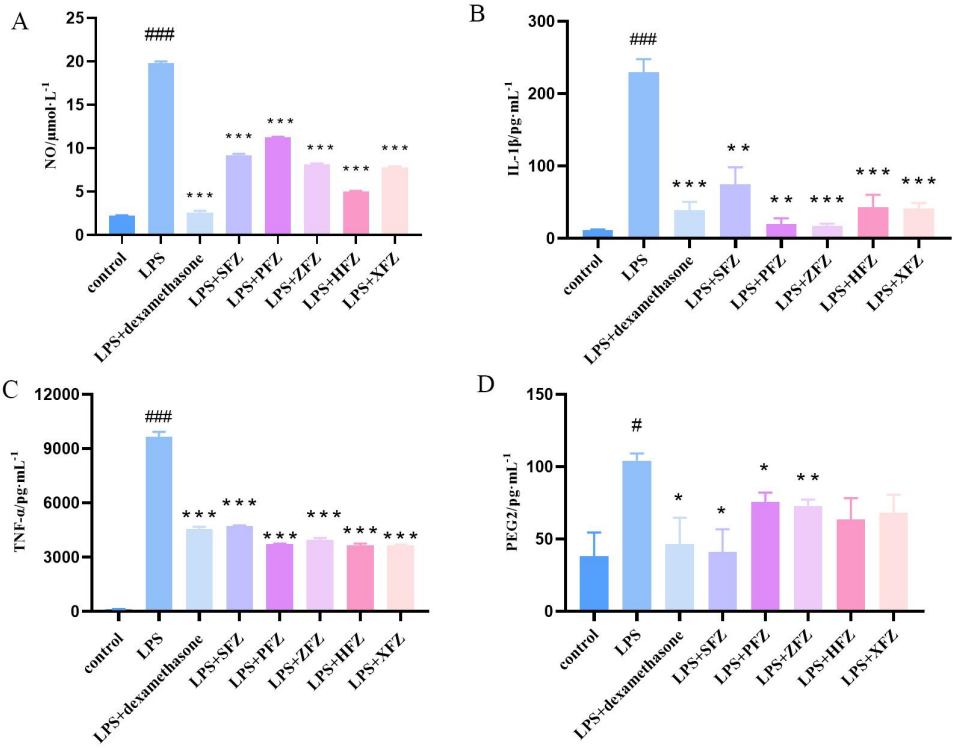

Figure 10 The anti-inflammatory impact of Fu-zi on LPS-stimulated RAW264.7 macrophages was evaluated. (A) NO. (B) IL-1β. (C) TNF-α. (D) PEG2. NO levels were quantified using the Griess reagent, while the production of IL-1β, TNF-α, and PGE2 cytokines was measured via ELISA kits and a microplate reader. The data are presented as means ± SEM (n = 3). ($^{*}P < 0.05$, $^{**}P < 0.01$ and $^{***}P < 0.001$ vs. LPS group, and $^{\#}P < 0.05$, $^{\#\#\#}P < 0.001$ vs. control group).

Pharmacology Discovery 2024;4(2):10. https://doi.org/10.53388/PD202404010

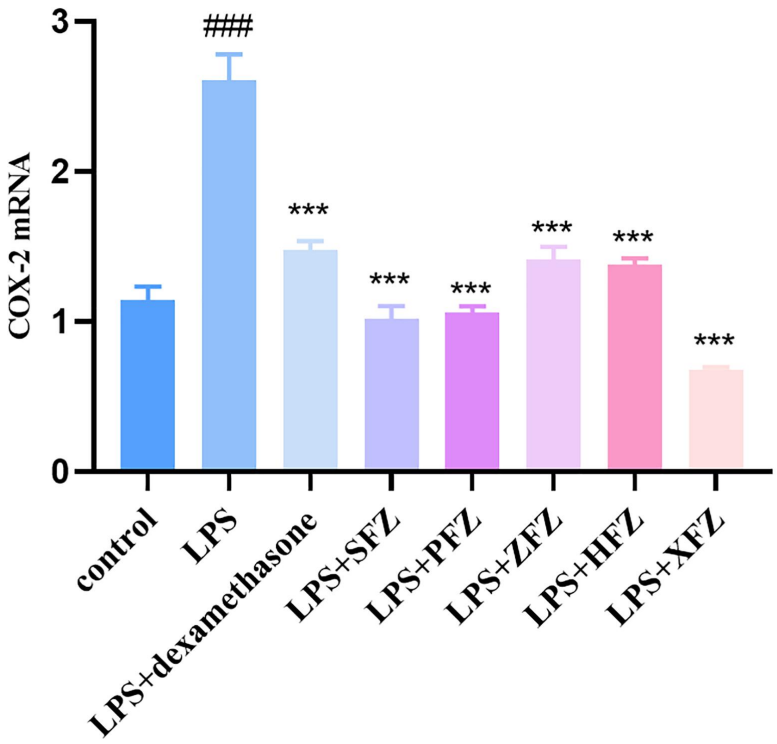

Figure 11 The mRNA levels of COX-2 were measured by qRT-PCR. The data are presented as means ± SEM (n = 4). ($^{***}P < 0.001$ vs. LPS group, and $^{###}P < 0.001$ vs. control group).

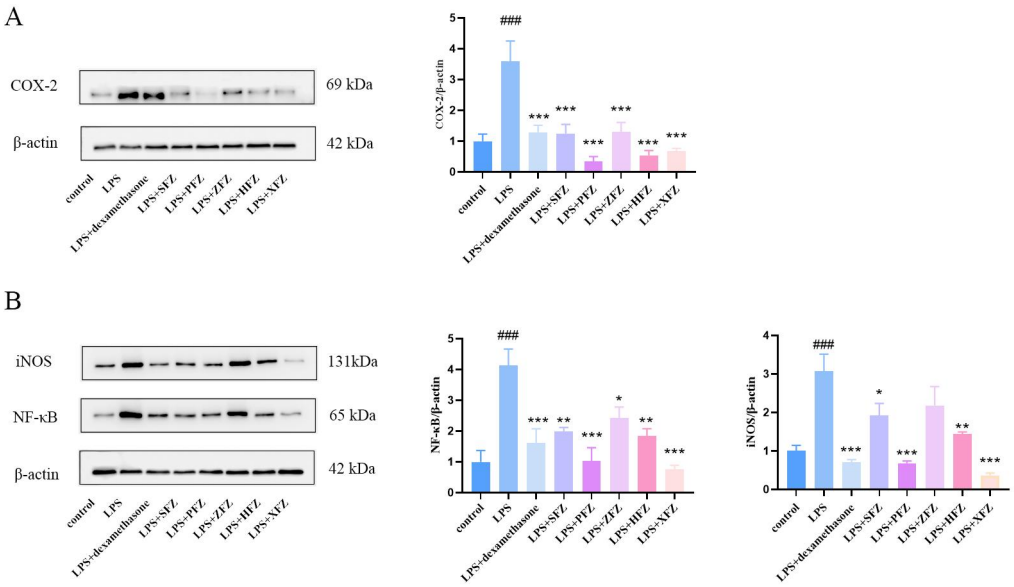

Figure 12 Protein expression of the anti-inflammatory effects of Fu-zi on LPS-induced RAW264.7 macrophages. (A) COX-2. (B) iNOS and NF-κB. The data are presented as means ± SEM (n = 3). ($^{*}P < 0.05$, $^{**}P < 0.01$ and $^{***}P < 0.001$ vs. LPS group, and $^{###}P < 0.001$ vs. control group).

Chronic inflammation is now recognized as an underlying pathological condition that can lead to hypofunction, dementia, osteoporosis, cancer, and other chronic diseases, thus exerting negative effects in healthy life expectancy [45]. Due to the obvious side effects of steroid and non-steroidal anti-inflammatory drugs, natural products have gained significant attention in the development of anti-inflammatory drugs [46]. Recent studies have shown that network pharmacology is a comprehensive approach with which to study the interactions between herbs, ingredients, diseases and their targets in TCM [47]. In an earlier investigation, Yang and colleagues employed network pharmacology and comprehensive metabolomic profiling to pinpoint PTGS2 as a likely pivotal therapeutic target for RA [48]. PTGS2 (as known as COX-2) is also a regulator of arachidonic acid metabolism and is involved in pro-inflammatory pathways. This is consistent with the results of our study in that PTGS2 was identified as one of the key targets of RA. Previous research has indicated that PTGS2, also known as COX-2, is highly inducible and can be rapidly upregulated in response to a variety of inflammatory stimuli [49]. PGE2 is one of the most abundant prostaglandins generated by COX-2 [50]. Other researchers have shown that the COX-2/PGE2 axis can significantly induce the migration and invasion of PC-3 cells [51].

NO, TNF-α, IL-1, and IL-6 are produced by active macrophages and

are considered to represent significant inflammatory cytokines in RA; these factors are known to be involved in the development of inflammation and joint destruction [52]. RAW264.7 macrophages can be used as an excellent *in vitro* model of inflammation [53]. Numerous cellular inflammatory cytokines, including NO, iNOS, PGE 2, COX-2, ILs, and TNF-, were released by LPS-induced RAW264.7 macrophages in the present study; these events lead to tissue damage and inflammation [54, 55]. The findings of the current investigation demonstrated that FPPs can significantly inhibit the release of NO, IL-1β, TNF-α, and PGE2, and that their inhibitory effects varied in an FFP-dependent manner. Western blotting results showed that FPPs could significantly down-regulate the protein levels of iNOS, COX-2 and NF-κB. On the other hand, the mRNA expression of COX-2 was significantly and differentially reduced by different FPPs, especially XFZ (the aqueous extract of Fu-zi prepared in strict accordance with the processing method of Fu-zi in ancient classical prescriptions). Therefore, our findings suggested that the five FPPs exerted anti-inflammatory activity by repressing the COX-2/PGE2 signaling pathway (shown in Figure 13), and that the anti-inflammatory effect of fu-zi prepared by the ancient processing method is better. This provides experimental evidence for subsequent studies focusing on the pharmacodynamical basis and quality control of fu-zi.

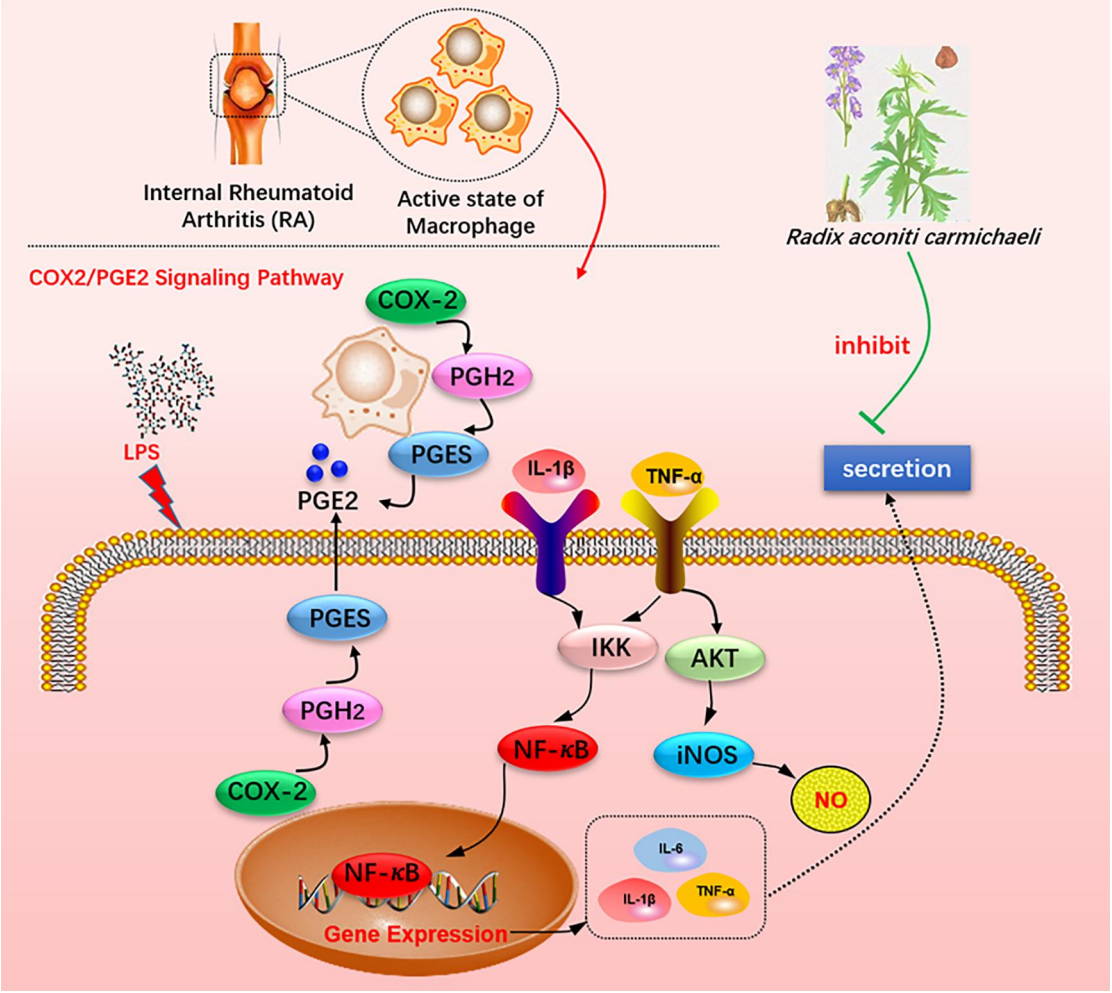

Figure 13 The anti-inflammatory mechanisms of Fu-zi through COX-2/PGE2 signaling pathways

Conclusions

In the current study, the underlying mechanism of five FPPs as anti-inflammatory agents has been further elucidated. The anti-inflammatory effects of the different FPPs in LPS-stimulated RAW264.7 macrophage cells were achieved *via* suppression of the COX-2/PGE2 signaling pathway, thus resulting in the reduced production of pro-inflammatory mediators and cytokines. Moreover, the anti-inflammatory effect of fu-zi prepared by the Chinese ancient traditional processing method was clearly better. However, further identification of the active ingredients of fu-zi is now required in order for it to developed as a natural pharmaceutical agent.

References

1. Arulselvan P, Fard MT, Tan WS, et al. Role of Antioxidants and Natural Products in Inflammation. *Oxid Med Cell Longev.* 2016;2016:1–15. Available at: http://doi.org/10.1155/2016/5276130
2. Fleit H. *Pathobiology of Human Disease: A Dynamic Encyclopedia of Disease Mechanisms*. Amsterdam, Netherlands: Elsevier; 2014.
3. Herold K, Mrowka R. Inflammation-Dysregulated inflammatory response and strategies for treatment. *Acta Physiol (Oxf).* 2019;226(3):e13284. Available at: http://doi.org/10.1111/apha.13284
4. Medzhitov R. Inflammation 2010: New Adventures of an Old Flame. *Cell.* 2010;140(6):771–776. Available at: http://doi.org/10.1016/j.cell.2010.03.006
5. Takeuchi O, Akira S. Pattern Recognition Receptors and Inflammation. *Cell.* 2010;140(6):805–820. Available at: http://doi.org/10.1016/j.cell.2010.01.022
6. Wang R, Zhou M, Ma H, et al. The Role of Chronic Inflammation in Various Diseases and Anti-inflammatory Therapies Containing Natural Products. *Chemmedchem.*

2021;16(10):1576–1592. Available at: http://doi.org/10.1002/cmdc.202000996
7. Díaz-González F, Hernández-Hernández MV. Rheumatoid arthritis. *Med Clin (Barc).* 2023;161(12):533–542. Available at: http://doi.org/10.1016/j.medcli.2023.07.014
8. Petrovská N, Prajzlerová K, Vencovský J, et al. The pre-clinical phase of rheumatoid arthritis: From risk factors to prevention of arthritis. *Autoimmun Rev.* 2021;20(5):102797. Available at: http://doi.org/10.1016/j.autrev.2021.102797
9. Fu L, Zhou XP, Li GC, et al. The Real World Study on Evaluating the Effect of Chinese Medicine Combined Western Medicine in Treating Rheumatoid Arthritis. *Chin J Integr Tradit West Med.* 2016;36(11):1319–1322. Available at: http://doi.org/10.7661/CJIM.2016.11.1319
10. Brown P, Pratt AG, Hyrich KL. Therapeutic advances in rheumatoid arthritis. *BMJ.* 2024;384:e070856. Available at: http://doi.org/10.1136/bmj-2022-070856
11. Commission CP. *National Pharmacopoeia Committee Pharmacopoeia of the people's Republic of China*. Beijing, China: China Medical Science and Technology Press; 2020.
12. Murayama M, Mori T, Bando H, et al. Studies on the constituents of Aconitum species. IX. The pharmacological properties of pyro-type aconitine alkaloids, components of processed aconite powder 'kako-bushi-matsu': analgesic, antiinflammatory and acute toxic activities. *J Ethnopharmacol.* 1991;35(2):159–164. Available at: http://doi.org/10.1016/0378-8741(91)90068-o.
13. Nyirimigabo E, Xu Y, Li Y, et al. A review on phytochemistry, pharmacology and toxicology studies of Aconitum. *J Pharm Pharmacol.* 2014;67(1):1–19. Available at: http://doi.org/10.1111/jphp.12310
14. Lei H, Zhang Y, Ye J, et al. A comprehensive quality evaluation of Fuzi and its processed product through integration of UPLC-QTOF/MS combined MS/MS-based mass spectral molecular networking with multivariate statistical analysis and HPLC-MS/MS. *J Ethnopharmacol.* 2021;266:113455. Available at: http://doi.org/10.1016/j.jep.2020.113455
15. Luo Z, Xia LY, Tang YQ, et al. Action Mechanism Underlying Improvement Effect of Fuzi Lizhong Decoction on Nonalcoholic Fatty Liver Disease: A Study Based on Network Pharmacology and Molecular Docking. *Evid Based Complement Alternat Med.* 2022;2022:1670014. Available at: http://doi.org/10.1155/2022/1670014.
16. Chen X, Wang R, Meng W, et al. Exploration of the Molecular Mechanism of FUZI (*Aconiti Lateralis Radix Praeparata*) in Allergic Rhinitis Treatment Based on Network Pharmacology. *Med Sci Monit.* 2020;26:e920872. Available at: http://doi.org/10.12659/MSM.920872
17. Sun F, Huang Y, Li L, et al. PKA/β2-AR-Gs/Gi signaling pathway is associated with anti-inflammatory and pro-apoptotic effects of Fuzi and Banxia combination on rats subjected to pressure overload. *J Ethnopharmacol.* 2019;235:375–384. Available at: http://doi.org/10.1016/j.jep.2019.02.011
18. Feng W, Liu J, Zhang D, et al. Revealing the efficacy-toxicity relationship of Fuzi in treating rheumatoid arthritis by systems pharmacology. *Sci Rep.* 2021;11(1):23083. Available at: http://doi.org/10.1038/s41598-021-02167-5
19. Zhang R, Liu F, Zhang Q, et al. Intra-articular delivery system of methotrexate for rheumatoid arthritis therapy: An in-suit thermosensitive comprehensive gel of polysaccharide from *Aconitum carmichaelii* Debx. *Int J Biol Macromol.* 2023;244:124822. Available at: http://doi.org/10.1016/j.ijbiomac.2023.124822
20. Song HH, Song TC, Yang T, et al. High mobility group box 1 mediates inflammatory response of astrocytes via cyclooxygenase 2/prostaglandin E2 signaling following spinal cord injury. *Neural Regen Res.* 2021;16(9):1848. Available at: http://doi.org/10.4103/1673-5374.303039
21. Nakanishi M, Rosenberg DW. Multifaceted roles of PGE2 in inflammation and cancer. *Semin Immunopathol.* 2012;35(2):123–137. Available at: http://doi.org/10.1007/s00281-012-0342-8
22. Wang X, Wang ZY, Zheng JH, et al. TCM network pharmacology: A new trend towards combining computational, experimental and clinical approaches. *Chin J Nat Med.* 2021;19(1):1–11. Available at: http://doi.org/10.1016/S1875-5364(21)60001-8
23. Han B, Dai Y, Wu H, et al Cimifugin Inhibits Inflammatory Responses of RAW264.7 Cells Induced by Lipopolysaccharide. *Med Sci Monit.* 2019;25:409–417. Available at: http://doi.org/10.12659/MSM.912042
24. Linghu KG, Ma QS, Zhao GD, et al. Leocarpinolide B attenuates LPS-induced inflammation on RAW264.7 macrophages by mediating NF-κB and Nrf2 pathways. *Eur J Pharmacol.* 2020;868:172854. Available at: http://doi.org/10.1016/j.ejphar.2019.172854
25. Ru J, Li P, Wang J, et al. TCMSP: a database of systems pharmacology for drug discovery from herbal medicines. *J Cheminform.* 2014;6:13. Available at: http://doi.org/10.1186/1758-2946-6-13
26. Xu HY, Zhang YQ, Liu ZM, et al. ETCM: an encyclopaedia of traditional Chinese medicine. *Nucleic Acids Res.* 2018;47(D1):D976–D982. Available at: http://doi.org/10.1093/nar/gky987
27. Morgat A, Lombardot T, Coudert E, et al. Enzyme annotation in UniProtKB using Rhea. *Bioinformatics.* 2020;36(6):1896–1901. Available at: http://doi.org/10.1093/bioinformatics/btz817
28. Szklarczyk D, Gable AL, Lyon D, et al. STRING v11: protein–protein association networks with increased coverage, supporting functional discovery in genome-wide experimental datasets. *Nucleic Acids Res.* 2018;47(D1):D607–D613. Available at: http://doi.org/10.1093/nar/gky1131
29. Shannon P, Markiel A, Ozier O, et al. Cytoscape: A Software Environment for Integrated Models of Biomolecular Interaction Networks. *Genome Res.* 2003;13(11):2498–2504. Available at: http://doi.org/10.1101/gr.1239303
30. Zhou Y, Zhou B, Pache L, et al. Metascape provides a biologist-oriented resource for the analysis of systems-level datasets. *Nat Commun.* 2019;10(1):1523. Available at: http://doi.org/10.1038/s41467-019-09234-6
31. Fermi G, Perutz MF, Shaanan B, et al. The crystal structure of human deoxyhaemoglobin at 1.74 A resolution. *Journal of molecular biology.* 1984;175(2):159–174. Available at: http://doi.org/10.1016/0022-2836(84)90472-8
32. Lang J, Li L, Chen S, et al. Mechanism Investigation of Wuwei Shexiang Pills on Gouty Arthritis via Network Pharmacology, Molecule Docking, and Pharmacological Verification. *Evid Based Complement Alternat Med.* 2022;2022:2377692. Available at: http://doi.org/10.1155/2022/2377692
33. Zhang J, Zhou Y, Ma Z. Multi-target mechanism of Tripteryguim wilfordii Hook for treatment of ankylosing spondylitis based on network pharmacology and molecular docking. *Ann Med.* 2021;53(1):1091–1099. Available at: http://doi.org/10.1080/07853890.2021.1918345
34. Liu L, Guo H, Song A, et al. Progranulin inhibits LPS-induced macrophage M1 polarization via NF-κB and MAPK pathways. *BMC Immunol.* 2020;21(1):32. Available at: http://doi.org/10.1186/s12865-020-00355-y
35. Marrelli M, De Marco CT, Statti G, et al. Ranunculus species suppress nitric oxide production in LPS-stimulated RAW 264.7 macrophages. *Nat Prod Res.* 2022;36(11):2859–2863. Available at: http://doi.org/10.1080/14786419.2021.1920018
36. Zhu H, Tong S, Yan C, et al. Triptolide attenuates LPS-induced activation of RAW 264.7 macrophages by inducing M1-to-M2

repolarization via the mTOR/STAT3 signaling. *Immunopharmacol Immunotoxicol.* 2022;44(6):894–901. Available at: http://doi.org/10.1080/08923973.2022.2093738
37. Sun H, Ni B, Zhang A, et al. Metabolomics study on Fuzi and its processed products using ultra-performance liquid-chromatography/electrospray-ionization synapt high-definition mass spectrometry coupled with pattern recognition analysis. *Analyst.* 2012;137(1):170–185. Available at: http://doi.org/10.1039/C1AN15833C
38. Liu CC, Cheng ME, Duan HY, et al. Reasearch on evolution and transition of processing method of fuzi in ancient and modern times. *Chin J Chin mater Med.* 2014;39(7):1339–1344. Available at: http://doi.org/10.4268/cjcmm20140738
39. Zong X, Yan X, Wu JL, et al. Potentially Cardiotoxic Diterpenoid Alkaloids from the Roots of *Aconitum carmichaelii*. *J Nat Prod.* 2019;82(4):980–989. Available at: http://doi.org/10.1021/acs.jnatprod.8b01039
40. Jiao J, Yang Y, Wu Z, et al. Screening cyclooxygenase-2 inhibitors from Andrographis paniculata to treat inflammation based on bio-affinity ultrafiltration coupled with UPLC-Q-TOF-MS. *Fitoterapia.* 2019;137:104259. Available at: http://doi.org/10.1016/j.fitote.2019.104259
41. Wang CC, Chen LG, Yang LL. Inducible nitric oxide synthase inhibitor of the Chinese herb I. *Saposhnikovia divaricata* (Turcz.) Schischk. *Cancer letters.* 1999;145(1–2):151–157. Available at: http://doi.org/10.1016/S0304-3835(99)00248-7
42. Zhu L, Wu J, Zhao M, et al. Mdr1a plays a crucial role in regulating the analgesic effect and toxicity of aconitine by altering its pharmacokinetic characteristics. *Toxicol Appl Pharmacol.* 2017;320:32–39. Available at: http://doi.org/10.1016/j.taap.2017.02.008
43. Abdin M, Hamed YS, Akhtar HMS, et al. Antioxidant and anti-inflammatory activities of target anthocyanins di-glucosides isolated from *Syzygium cumini* pulp by high speed counter-current chromatography. *J Food Biochem.* 2020;44(6):e13209. Available at: http://doi.org/10.1111/jfbc.13209
44. Bose M, Chakraborty M, Bhattacharya S, et al. Prevention of Arthritis Markers in Experimental Animal and Inflammation Signalling in Macrophage by Karanjin Isolated fromPongamia pinnataSeed Extract. *Phytother Res.* 2014;28(8):1188–1195. Available at: http://doi.org/10.1002/ptr.5113
45. Suzuki K. Chronic Inflammation as an Immunological Abnormality and Effectiveness of Exercise. *Biomolecules.* 2019;9(6):223. Available at: http://doi.org/10.3390/biom9060223
46. Scheiman JM. NSAID-induced Gastrointestinal Injury. *J Clin Gastroenterol.* 2016;50(1):5–10. Available at: http://doi.org/10.1097/MCG.0000000000000432
47. Xiong Y, Hu Y, Chen L, et al. Unveiling Active Constituents and Potential Targets Related to the Hematinic Effect of Steamed *Panax notoginseng* Using Network Pharmacology Coupled With Multivariate Data Analyses. *Front Pharmacol.* 2019;9:1514. Available at: http://doi.org/10.3389/fphar.2018.01514
48. Yang J, Zhang Y, Li W, et al. Assessment of the anti-rheumatoid arthritis activity of Gastrodia elata (tian-ma) and *Radix aconitic lateralis preparata* (fu-zi) via network pharmacology and untargeted metabolomics analyses. *Int J of Rheum Dis.* 2021;24(3):380–390. Available at: http://doi.org/10.1111/1756-185X.14063
49. Tong D, Liu Q, Wang L, et al. The roles of the COX2/PGE2/EP axis in therapeutic resistance. *Cancer Metastasis Rev.* 2018;37(2–3):355–368. Available at: http://doi.org/10.1007/s10555-018-9752-y
50. Greenhough A, Smartt HJM, Moore AE, et al. The COX-2/PGE2 pathway: key roles in the hallmarks of cancer and adaptation to the tumour microenvironment. *Carcinogenesis.* 2009;30(3):377–386. Available at: http://doi.org/10.1093/carcin/bgp014
51. Ko CJ, Lan SW, Lu YC, et al. Inhibition of cyclooxygenase-2-mediated matriptase activation contributes to the suppression of prostate cancer cell motility and metastasis. *Oncogene.* 2017;36(32):4597–4609. Available at: http://doi.org/10.1038/onc.2017.82
52. Li G, Zhao J, Li B, et al. Associations between CCL21 gene polymorphisms and susceptibility to rheumatoid arthritis: a meta-analysis. *Rheumatol Int.* 2017;37(10):1673–1681. Available at: http://doi.org/10.1007/s00296-017-3784-4
53. Oh GS, Pae HO, Lee BS, et al. Hydrogen sulfide inhibits nitric oxide production and nuclear factor-kappaB via heme oxygenase-1 expression in RAW264.7 macrophages stimulated with lipopolysaccharide. *Free radic biol med.* 2006;41(1):106–119. Available at: http://doi.org/10.1016/j.freeradbiomed.2006.03.021
54. Dai JN, Zong Y, Zhong LM, et al. Gastrodin inhibits expression of inducible NO synthase, cyclooxygenase-2 and proinflammatory cytokines in cultured LPS-stimulated microglia via MAPK pathways. *PloS one.* 2011;6(7):e21891. Available at: http://doi.org/10.1371/journal.pone.0021891
55. Yuan L, Wu Y, Ren X, et al. Isoorientin attenuates lipopolysaccharide-induced pro-inflammatory responses through down-regulation of ROS-related MAPK/NF-κB signaling pathway in BV-2 microglia. *Mol Cell Biochem.* 2013;386(1–2):153–165. Available at: http://doi.org/10.1007/s11010-013-1854-9